Journal of Molecular Catalysis B: Enzymatic 56 (2009) 246–252

Contents lists available at ScienceDirect

Journal of Molecular Catalysis B: Enzymatic

journal homepage: www.elsevier.com/locate/molcatb

Effects of pH and pore characters of mesoporous silicas on horseradish peroxidase immobilization

Wilaiwan Chouyyok[a], Joongjai Panpranot[a], Chanchana Thanachayanant[b], Seeroong Prichanont[a,*]

[a] Department of Chemical Engineering, Faculty of Engineering, Chulalongkorn University, Phayathai Road, Bangkok 10330, Thailand
[b] National Metal and Materials Technology Center, Thailand Science Park, Paholyothin Road, Phatumthani 12120, Thailand

ARTICLE INFO

Article history:
Received 8 October 2007
Received in revised form 8 May 2008
Accepted 9 May 2008
Available online 15 May 2008

Keywords:
Enzyme immobilization
Mesoporous silica
Horseradish peroxidase

ABSTRACT

Effects of immobilization pH and pore characters of mesoporous silicas (MPSs), MCM-41, SBA-15, and MCF, were simultaneously investigated for the immobilization of horseradish peroxidase (HRP; EC 1.11.1.7). MCM-41 and SBA-15 were rod-like with respective average pore diameters of 32, and 54 Å, while that of MCF with spherical cell and frame structure was 148 Å. Moreover, the MPSs synthesized were of identical surface functional groups and similar contents of free silanol groups. At immobilization pH 6 and 8 almost 100% HRP loadings were obtained and insignificant leaching were observed for all types of supports at pH 6. However, MCF was found to give both the highest enzyme loading and leaching at pH 10. Maximum and minimum HRP activities were obtained at respective immobilization pH 8, and 6. Activities of immobilized HRP increased with support pore diameters in the order: MCM-41 < SBA-15 < MCF. HRP immobilized at pH 8 gave the highest storage stability (both at 4 °C and room temperature), and in opposition to pH 6. In addition, HRP immobilized in MCF was found to be the most stable under storage. The finding should be useful for the creation of biocatalysts and biosensors.

1. Introduction

Immobilization of enzymes on insoluble supports is of significant process due to its promising potential in improving enzyme thermal or pH stability, easing product purification, and facilitating enzyme recycling [1–7]. Therefore, immobilized enzymes are widely applied in the fields of biocatalysis and biosensors [8–12].

Among the various supports used for enzyme immobilization, mesoporous silicas (MPSs) are of considerable interests. Their main advantages are the tunable pore diameters in the range of 1–30 nm which are similar to sizes of enzyme molecules [13], high surface areas (~1000 m^2/g), ordered structures, high stability to chemical and mechanical forces, and resistance to enzyme attack [14]. Moreover, enzyme immobilization on these carriers can simply be achieved by physical adsorption which has the least effect on enzyme structures compared to other methods such as covalent bonding [15]. In addition, the existence of silanol groups on MPS surface possibly helps enhancing physical adsorption of enzymes via hydrogen bonding [16]. Therefore, MPSs have been extensively studied for immobilization of various enzymes [13–23]. It is generally reported that factors influencing enzyme immobilization are a pore diameter [7,13,16,18], and surface characteristics of MPSs [13,20–22]. Specifically, excellent thermal stability and high enzyme activities can be obtained when average support pore diameter matches that of enzyme molecular size. MCM-41, SBA-15 and MCF are among members of mesoporous silicas that have been widely used for biomolecular immobilization [13–23]. MCM-41 and SBA-15 possess cylindrical hexagonal structures while MCF has spherical cells and frame structure. Due to different template and/or synthesis conditions, these MPSs are of different pore sizes, surface areas, and surface charges. Thus, different immobilized enzyme activities and stability on these supports are undoubtedly expected.

Horseradish peroxidase (HRP, EC 1.11.1.7) was used as a model enzyme in this study due to its wide applications. HRP is a catalyst for oxidative reactions of many chemicals, for instance, phenols and polyphenols (i.e. phenolic acid, flavonoids, and tannins) [24–26]. Therefore, it has been used to verify contaminants in food and wastewater from oil industry, paints, polymer, and drug factories [27], and to indicate amounts of antioxidant compounds in food and beverages [28,29]. For HRP immobilization on MPSs, various factors such as support synthesizing procedure, pH and ionic strength of enzyme solution, and reaction or storage temperature were found to affect HRP adsorption or stability. Díaz and Balkus [17] reported that amounts of various proteins adsorbed on MCM-41 depended on their molecular sizes, thus HRP with relatively large molecular diameter was less adsorbed. Moreover, it was found that the

* Corresponding author. Tel.: +66 22186860; fax: +66 22186877.
E-mail address: seeroong.p@chula.ac.th (S. Prichanont).

1381-1177/$ – see front matter © 2008 Elsevier B.V. All rights reserved.
doi:10.1016/j.molcatb.2008.05.009

amount of adsorbed HRP was higher on supports synthesized from cationic surfactant (FSM-16 and MCM-41) than from nonionic surfactant (SBA-15) [13]. Some other factors such as pH [18,23] and ionic strength [5,30] of enzyme solution were also found to affect the degree of enzyme bonding on silica surface. For example, the maximum degree of protein bonding was observed at a pH closed to the protein's isoelectric point. Thermal stability of immobilized enzyme is another key parameter considered for further applications. Immobilized HRP on MCM-41 showed the highest thermal stability in aqueous solution at 70 °C in comparison to free HRP and HRP immobilized in silica gel [13]. Other reports also disclosed that thermal stability of immobilized HRP on various supports was apparently higher than that of free enzyme [2,3]. Although MPSs have been demonstrated to be favorable for stabilizing HRP, effects of immobilization pH and MPS pore characters on enzyme immobilization are still unclear.

Thus, in this work we aimed at addressing these effects of immobilization pH and MPS pore characters on HRP immobilization. MPSs with different pore characters and surface charges namely; MCM-41, SBA-15, and MCF were selected for the study. It is revealed in this paper that both immobilization pH and MPS pore characters play significant and interactive roles on enzyme loading, leaching, activity, and storage stability. The finding should be useful for the creation of biocatalysts and biosensors.

2. Materials and methods

2.1. Materials

Horseradish peroxidase (EC 1.11.1.7) was purchased from Toyobo Co. Ltd. (266 U/mg; 1 U was defined as the formation of 1 mg of purpurogallin in 20 s in phosphate buffer pH 6.0, at 20 °C with 5% (w/v) pyrogallol solution, and 0.147 mM H_2O_2 solution). Hexadecytrimethyl-ammonium bromide (CTABr, 99%) was obtained from Sigma. Pluronic P123 was procured from BASF. Ludox As-40 colloidal silica (40 wt.%) and tetraethoxysilane (TEOS, 98%) were purchased from Sigma–Aldrich. 1,3,5-Trimethylbenzene (TMB) was purchased from Supelco. Ammonium solution (NH_3) was obtained from Carlo Erba. Acetic acid (CH_3COOH) and conc. hydrochloric acid (HCl) were purchased from J.T. Baker. Pyrogallol was procured from POCH. Hydrogen peroxide (30%) was obtained from Polskie Opczynniki Chemiczne S.A.

2.2. Syntheses of MPSs

Three types of silica supports were synthesized: MCM-41, SBA-15, and MCF. Brief description of the syntheses is given below.

MCM-41 was synthesized according to the method reported by Cho et al. [31] which consisted of two solutions: A and B. Solution A was prepared by adding 12.15 g CTABr to 36.46 g deionized water, rigorous stirring was done to homogeneity. Next, 0.4 g of 25% NH_3 solution was added, and the solution was again stirred for 30 min at room temperature (30 ± 2 °C). Solution B which consisted of 2.66 g NaOH, 71.41 g deionized water, and 20.30 g Ludox was then added to solution A. After being mixed to homogeneity, the solution was poured into a Teflon bottle which its lid was then closed tightly. The mixture was aged at 100 °C for 5 days, during this time its pH was adjusted daily to 10.2 with 30% CH_3COOH solution. After aging, the obtained particles were subsequently filtered and washed once with deionized water. The synthesized particles were dried at 100 °C for 16 h. The surfactant template was then removed by calcination at 540 °C for 6 h.

SBA-15 was synthesized using the method proposed by Zhao et al. [32]. Pluronic P123 (4 g) was dissolved in 30 g of water and 120 g of 2 M HCl. Then, 8.50 g TEOS was added to the solution which was next stirred at room temperature for 20 h. The obtained mixture was poured into a Teflon bottle, and aged at 80 °C for 24 h. The particles achieved were filtrated and washed with deionized water until the filtrate pH was similar to that of deionized water. The synthesized material was subsequently dried at room temperature. Later, the template was removed by calcination at 500 °C for 6 h.

MCF preparation was initiated by dissolving 2 g Pluronic P123 in 75 mL of 1.6 M HCl at 35–40 °C [33]. Then, 1 g of TMB was added to the solution, and the mixture was stirred to homogeneity. Succeedingly, 4.25 g TEOS was added, and the mixture was continuously stirred at 35–40 °C for 24 h. The solution was next aged at 100–120 °C for 24 h. MCF was finally obtained using the same procedures as described for SBA-15.

2.3. Characterization of MPSs

Characterizations of MPSs were achieved by N_2-adsorption, XRD, TEM, FTIR, and Zeta potential measurement. The adsorption–desorption isotherms were obtained at 77 K using a Micromeritics ASAP 2020 automated system. The surface area was determined using Brunauer–Emmett–Teller (BET) method. The main pore diameter and pore volume of supports were obtained from the adsorption isotherm branch data and Barret–Joyner–Halenda (BJH) method. The structure of mesoporous silica supports was analyzed using X-ray diffractometer (XRD; Bruker AXS Model D8 Discover), and Transmission electron microscope (TEM; JEOL JEM 2010). Surface properties of supports were analyzed by Fourier transform infrared spectrometer (FTIR; Thermo scientific Nicollet 6700), and Zeta potential was measured by Zetasizer Nano (Malvern ZS 90).

2.4. Enzyme immobilization and enzyme leaching

To immobilize HRP on MPSs, an amount of 0.4 g MPS was added to 8 mL of 0.1 mg mL^{-1} enzyme solution of specified pH (pH 6, 8, and 10). The mixture was subsequently gently stirred at 4 °C for 24 h then the solid was filtered and washed with the same buffer to remove unattached enzyme. The solid was taken for an assay of immobilized enzyme activity.

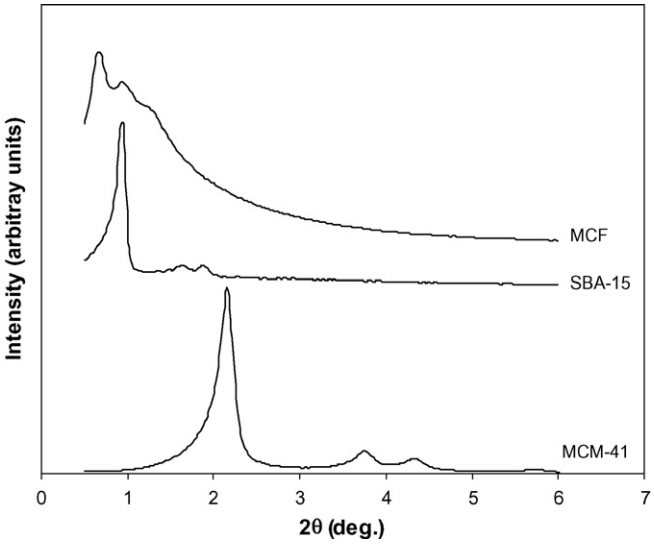

Fig. 1. Powder XRD patterns of mesoporous silicas: MCM-41, SBA-15, and MCF.

Enzyme leaching was tested by adding 0.05 g of HRP contained MPS to 1 mL of a buffer solution of the same pH specified in the immobilization process. The mixture was next stirred at 300 rpm at room temperature ($30 \pm 2\,^{\circ}C$) for 2 h. Then the buffer solution was analyzed for free enzyme activity.

$$\text{enzyme loading}(\%) = \frac{\text{activity of initial enzyme in buffer solution} - \text{activity of free enzyme remained in buffer solution}}{\text{activity of initial enzyme in buffer solution}} \times 100$$

$$\text{enzyme leaching}(\%) = \frac{\text{activity of leached enzyme in buffer solution}}{\text{activity of initially loaded enzyme}} \times 100$$

2.5. Storage stability test

The immobilized HRP on MPSs were kept in closed containers, and stored at room temperature ($30 \pm 2\,^{\circ}C$) and $4\,^{\circ}C$ for a specified period of time without humidity control. Subsequently, 0.002 g of stored HRP contained MPSs was taken for activity assay.

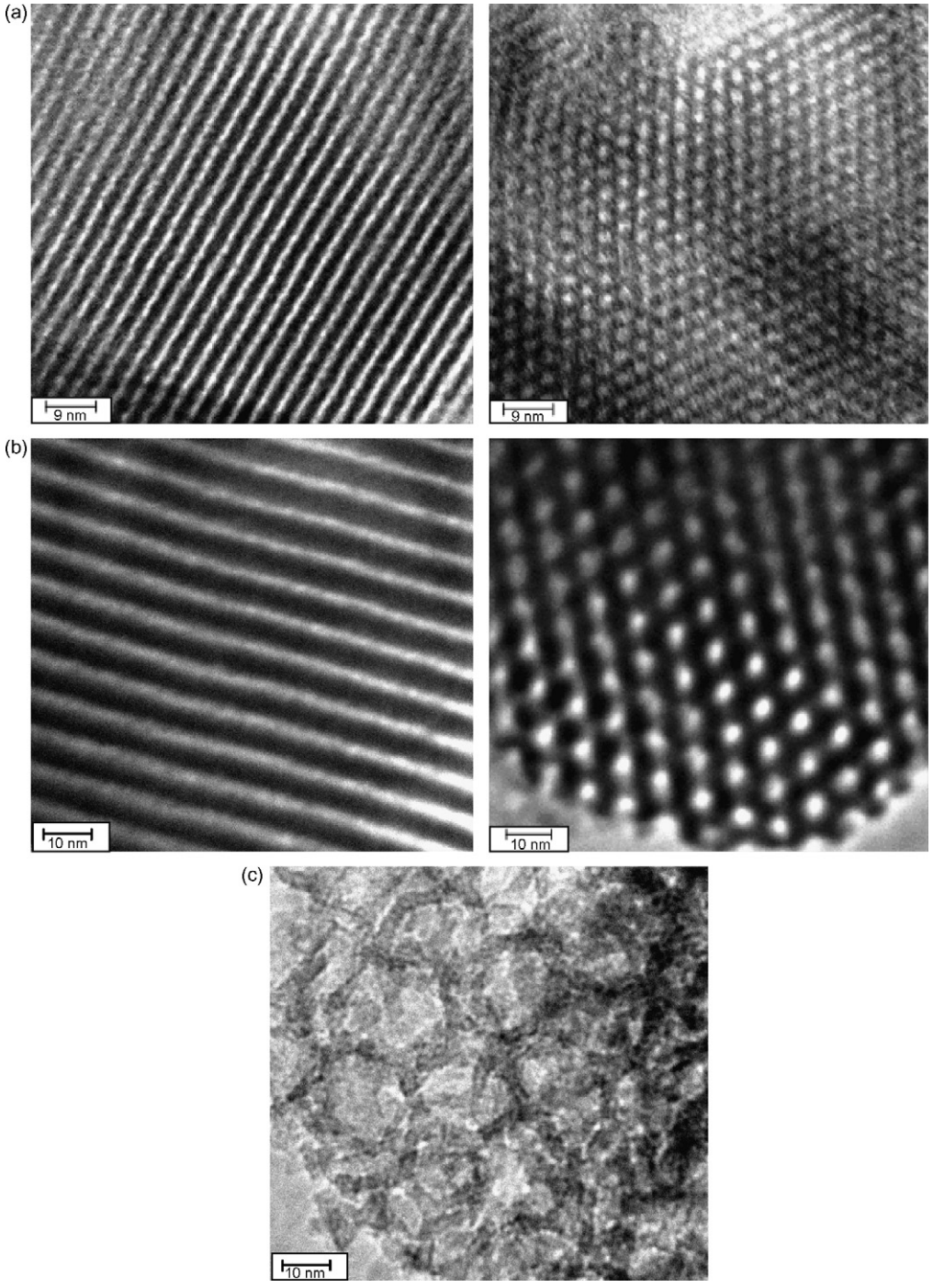

Fig. 2. TEM images of mesoporous silicas: (a) MCM-41 observed perpendicular (left) and parallel (right) to the pores; (b) SBA-15 observed perpendicular (left) and parallel (right) to the pores; (c) MCF.

$$\text{residual activity}\,(\%) = \frac{\text{activity of immobilized enzyme at specified storage time}}{\text{activity of immobilized enzyme before storage}} \times 100$$

2.6. Assay of free and immobilized enzyme

The analysis of free HRP was achieved using two substrates which were hydrogen peroxide and pyrogallol in a reaction according to Halpin et al. [34]. The reaction was initiated by an addition of 0.5 mL hydrogen peroxide (0.05 M) to a mixture of 2.4 mL phosphate buffer solution (pH 6.0) containing 0.013 M pyrogallol, and 0.1 mL of a buffer solution (with the same pH of the immobilization process) containing 0.002 mg HRP. The reaction was carried out at 30 °C for 1 min after which the absorbance of the product (purpurogallin) was measured at 420 nm using a spectrophotometer (spectronic® 20 Genesys™). The extinction coefficient of pyrogallol was found to be 0.0126 M^{-1} cm^{-1} at 420 nm.

The assay of immobilized HRP was performed under similar conditions as those of free enzyme except that free HRP was replaced with 0.002 g of HRP contained MPSs. All samples were analyzed in triplicate. One unit of HRP activity was defined as the formation of 1 μmol of purpurogallin in 1 min at pH 6.0, and 30 °C.

3. Results and discussion

3.1. Support characteristics and HRP immobilization

Characteristics of MPSs as enzyme supports are important information for understanding enzyme immobilization and their activities. XRD patterns of the calcined MCM-41, SBA-15, and MCF are shown in Fig. 1. MCM-41 and SBA-15 exhibited highly distinct patterns at low 2θ angles reflecting the ordered hexagonal mesoporous structures [16]. On the other hand, the primary XRD characteristic peak of MCF was not resolved from others suggesting different mesoporous structure. TEM micrographs of all the supports as shown in Fig. 2 confirmed the hexagonal structures and long cylindrical pores of MCM-41 and SBA-15 whereas the spherical cells and frame structure were observed for MCF. Structure parameters of MPSs were evaluated through the nitrogen adsorption isotherms using the BET, and BJH methods. Pore size distributions of the synthesized supports are shown in Fig. 3. As expected, MCM-41 and SBA-15 possessed very narrow main pore size distributions which were dissimilar to MCF. Table 1 shows main pore diameters and pore volumes as well as BET surface areas of the three supports. MCM-41, SBA-15, and MCF had the main pore diameters of 32, 54, and 148 Å, respectively, while the elongated shape HRP molecule had the approximated respective long and short axes of 64, and 37 Å [35]. The reduction in surface area, and pore volume after HRP immobilization for all the MPSs was most likely attributed to the adsorption of HRP inside the mesopores. The fact that HRP molecules were able to diffuse into the channels of MCM-41 even of their slightly bigger sizes than the main pore diameter was also evidenced by Yiu et al. [16] for trypsin immobilization in MCM-41. The slight decreases in main pore diameters of MCM-41, and SBA-15 after HRP immobilization suggested that some HRP were immobilized on the pore mouths of the supports [36]. The schematic diagrams representing HRP allocation in/on mesoporous silica supports are proposed in Fig. 4. For MCM-41, only a small amount of HRP could occupy the mesoporous space due to the relatively small main entrance sizes of the pores in comparison to HRP molecular size. Therefore, most of the enzyme molecules were expected to be adsorbed on the external surface. This assumption was evidently confirmed by slight decreases of BET surface area and pore volume of MCM-41 after HRP immobilization (decreased by 18.0% and 14.6%, respectively). Since the main pore diameter of SBA-15 was comparable to the dimensions of enzyme molecules, HRP was easier adsorbed in the pores. Large decreases in BET surface area and pore volume of SBA-15 (42.4% and 36.6%, respectively) were therefore observed after HRP immobilization. MCF which contained the largest main pore diameter and pore volume among the three supports undoubtedly allowed comfortable entrapment of HRP in the pores. The BET surface area and pore volume of MCF decreased by 34% and 10%, respectively after HRP immobilization. A slight decrease of MCF pore volumes was probably due to its initially larger pore volume compared to MCM-41 and SBA-15.

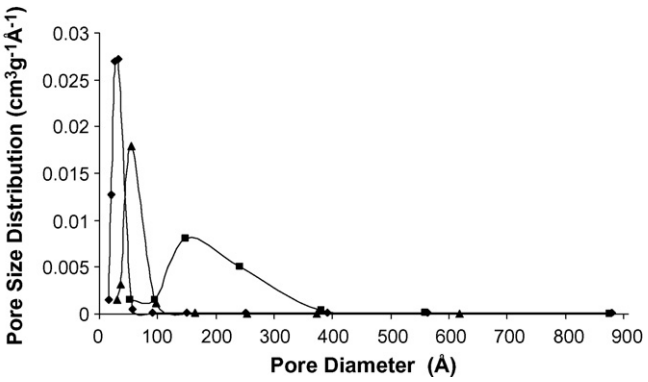

Fig. 3. Pore size distribution of mesoporous silicas: (♦) MCM-41, (▲) SBA-15, and (■) MCF.

Fig. 5 shows FTIR spectra of MCM-41, SBA-15, and MCF. The band between 3700 and 3200 cm^{-1} is attributed to Si–OH stretching (silanol group), while between 1200–1000 cm^{-1} and at 1630 cm^{-1} are shown respectively for siloxane, $-(Si-O)_n-$, and water molecules. The similar trends of FTIR spectra observed for the three MPSs indicated identical surface functional groups. Moreover, the Si–OH/Si–O area ratios (area ratios of Si–OH/Si–O were 0.8477, 0.8229, and 0.8320 for MCM-41, SBA-15, and MCF, respectively) were comparable suggesting similar contents of free silanol groups among these supports [36]. Hence, resemble interactions between immobilized HRP and surfaces of different MPSs are expected.

3.2. HRP loading and leaching

In this work, two parameters influencing HRP immobilization namely; immobilization pH (pH of the buffer solution used in the immobilization step) and support pore characters were simultane-

Table 1
Pore characteristics of MCM-41, SBA-15, and MCF before and after HRP immobilization

Supports	Main pore diameter (Å)		BET surface (m^2 g^{-1})		Pore volume (cm^3 g^{-1})	
	Before	After	Before	After	Before	After
MCM-41	32	27	888	724	0.84	0.71
SBA-15	54	52	798	460	1.06	0.67
MCF	148	148	618	408	1.60	1.44

Calculated from adsorption branch of the N_2 isotherm.

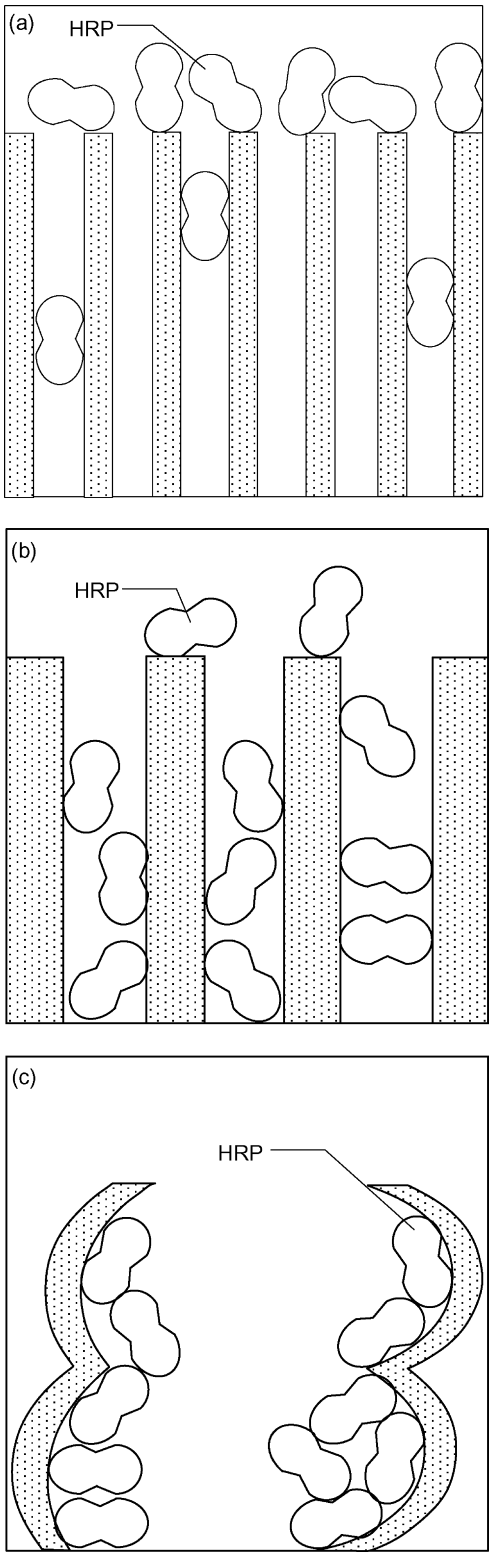

Fig. 4. Schematic diagram of immobilized HRP in (a) MCM-41, (b) SBA-15, and (c) MCF.

ously investigated. The effect of immobilization pH on HRP loading is shown in Fig. 6. At immobilization pH equaled to or lesser than 8, the net charge of the enzyme was positive (p*I* ~ 8.9) while that of the support surface was negative (p*I* of silica ~2). Thus, high electrostatic attractions were obtained which led to almost 100%

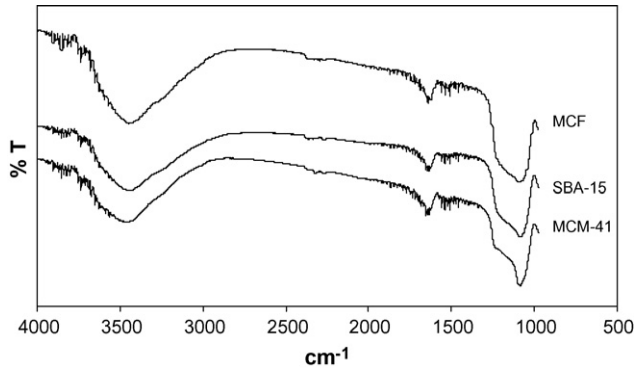

Fig. 5. FTIR of calcined mesoporous silicas: MCM-41, SBA-15, and MCF.

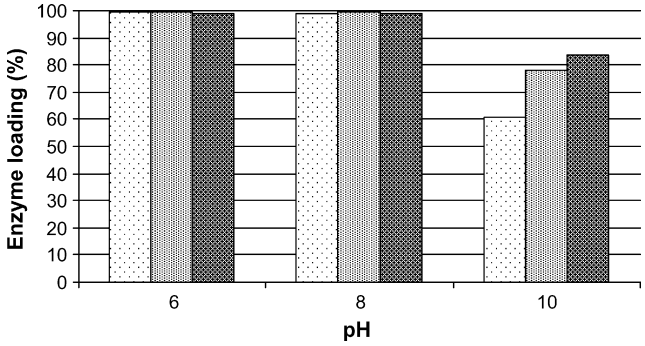

Fig. 6. Effects of immobilization pH and types of silicas on HRP loading: MCM-41 (□), SBA-15 (▨), and MCF (■).

of enzyme loading at pH 6 and 8 for all types of supports investigated. This is in accordance to Rezwan et al. [37] who studied the influence of surface charge on the adsorbed amount of lysozyme and bovine serum albumin on silica particles. They concluded that the amount of adsorbed protein strongly corresponds to the sign of the net charge of the protein and of the particle surface. The reason that MCM-41 was able to exhibit comparable enzyme loading capacity even of its small main pore diameter might be due to its notably higher surface area, and improved anionic potential of the silanol group on the pore surface owing to the use of cationic surfactant as a template [13]. This is confirmed by the zeta-potential data reported in Table 2. It is demonstrated that MCM-41 held higher negative charges than other supports (synthesized using nonionic surfactant as templates) at every pH. At pH 10, both the enzyme and support surfaces possessed net negative charges, therefore only between 60 and 84% HRP loading were attained. At this pH, it is obvious that the effect of support main pore size was more pronounced than electrostatic interactions. Significant amount of HRP molecules could still be loaded into pores of MCF even under electrostatic repulsions. The results in this study, however, emphasized that adjustment of enzyme immobilization pH can significantly enhance amounts of enzyme adsorbed on the supports, regardless of the types of surfactant template used.

The amount of enzyme leaching also depends on pore characters of support and interactions between enzyme and support surfaces.

Table 2
Zeta-potential (mV) of silica support surface in different pH solutions

pH/support	MCM-41	SBA-15	MCF
6	−8.17	−5.54	−7.738
8	−17.46	−11.53	−14.90
10	−27.17	−21.27	−25.32

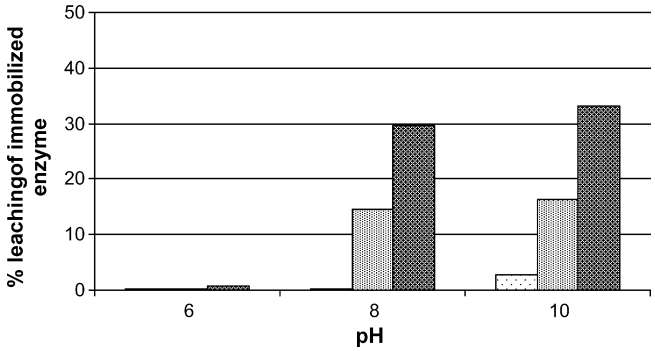

Fig. 7. Effects of immobilization pH and types of silicas on HRP leaching: MCM-41 (□), SBA-15 (▨), and MCF (▩).

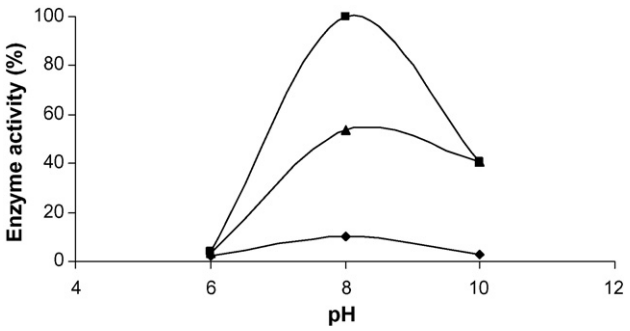

Fig. 8. Effects of immobilization pH and types of silicas on HRP activity: (♦) MCM-41, (▲) SBA-15, and (■) MCF.

It is clearly seen in Fig. 7 that immobilized HRP was leached out from MCF, with a large main pore diameter and of spherical cells and frame structure, in a greater extent than smaller and long cylindrical pores of SBA-15 and MCM-41, especially at relatively high pH (pH 8 and 10). This is in accordance to Lin et al. [38] who found that HRP leaching from silica materials increased with increasing pore size. This demonstrates significant effects of support pore characters on enzyme leaching. At pH 6, leaching of enzyme from all supports was negligible. This underpins our assumption that charges of HRP molecule and support surface have strong influence on their attachment. At this pH, their attractive interactions were very strong therefore less leaching was observed. The interactions

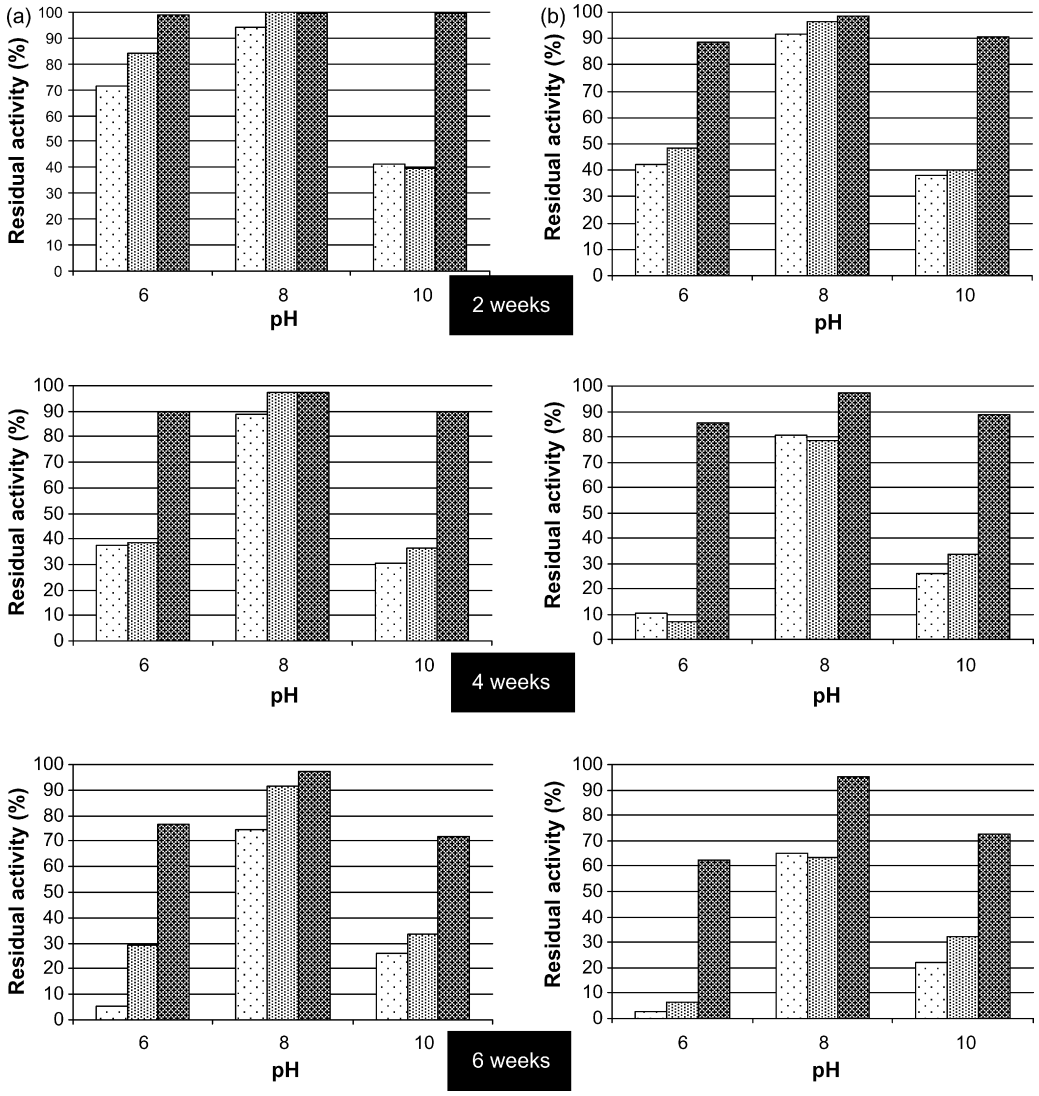

Fig. 9. Effects of immobilization pH and types of silicas on HRP storage stability: (a) at 4 °C, and (b) at room temperature (30 ± 2 °C): (□) MCM-41, (▨) SBA-15, and (▩) MCF.

became weaker as pH increased. However, for a given support type, the amounts of leached enzyme were not significantly different comparing between pH 8 and 10.

3.3. HRP activity and stability

Effects of immobilization pH and support pore characters on immobilized HRP activity are demonstrated in Fig. 8. Under the same reaction pH 6, immobilization pH appeared to be a pivotal parameter governing immobilized enzyme reaction. Maximum and minimum specific activities were obtained from immobilization pH of 8 and 6, respectively, for all support types. This is surprising since free HRP was reported to be most active at pH 6. We postulated that strong electrostatic attractions between high negatively charged silica and high positively charged enzyme at pH 6 caused inflexible HRP molecules or hindered enzyme active sites thus hampered their activities. Caramori and Fernandes [2] also reported that immobilized HRP onto polymer composite material was less active at pH 6 than other pH. The activity of immobilized enzyme on different silica supports was in the order: MCF > SBA-15 > MCM-41. The obtained results are in accordance to the literature that wider pore diameters facilitate substance mass-transfer to and from enzyme active sites. In addition, MCF structure of spherical cells and frame was anticipated to be more suitable for mass-transfer than long cylindrical structures of SBA-15 and MCM-41. The maximum specific activity obtained from immobilized HRP on MCF was ca. 30% of free enzyme. This suggests that a part of HRP was denatured during immobilization or was inaccessible to the substrate. Moreover, Carrado et al. [39] postulated that the chemical nature of the material's surface could modify the enzyme conformation to a less active one. The results obtained in this report indicated the significance of electrostatic interaction effect over the effects of support pore characters on immobilized enzyme activity.

Storage stability of immobilized HRP was evaluated every 2 weeks after the enzyme was kept in dried form at 4 °C and room temperature (see Fig. 9). It is evident that HRP immobilized at pH 8 had the highest storage stability, in contrast to pH 6 which gave the lowest stability. Lower electrostatic interactions between enzyme and support occurred to be better for enzyme storage. These phenomena were true for both storage temperatures and for all types of supports. This indicates that electrostatic interaction was one of the key parameters influencing storage stability of the enzyme. Equally important were the support pore characters, since it was found that storage stability of immobilized HRP in MCF was much greater than in MCM-41. Supports with bigger main pore diameters appeared to be better for enzyme storage stability than those with smaller pores. The conclusions may be drawn here that HRP is likely to be denatured under conditions that rigidly control its three-dimensional structure and the denaturation increases with storage time.

4. Conclusions

The experimental results obtained in the present work revealed significant roles of electrostatic interactions and MPSs pore characters on enzyme loading, leaching, activity, and storage stability. MCM-41 and SBA-15 were rod-like with respective main pore diameters of 32, and 54 Å, while that of MCF with spherical cell and frame structure was 148 Å. Under attractive interactions (at immobilization pH 6 and 8) almost 100% HRP loadings were obtained for all types of supports. However, effects of pore characters were more pronounced under repulsive interactions at immobilization pH 10. In this case, MCF which was of the biggest pore diameters gave both the highest enzyme loading and leaching. Insignificant HRP leaching was observed at immobilization pH 6 for all types of supports.

Maximum and minimum HRP activities were obtained at respectively immobilization pH 8 and 6. Inflexibility of HRP molecules at pH 6 or hindered enzyme active sites were postulated to be reasons for the low enzyme activity. It was found that activities of immobilized HRP increased with support pore diameters in the order: MCM-41 < SBA-15 < MCF. HRP immobilized at pH 8 had the highest storage stability (both at 4 °C and room temperature), and in opposition to pH 6. In addition, HRP immobilized in MCF was the most stable under storage. It was therefore hypothesized that HRP was likely to be denatured under conditions that rigidly control its three-dimensional structure. The conclusions drawn in this work may be significant for the understanding of enzyme immobilization in mesoporous silicas and undoubtedly useful for their applications in the fields of biocatalysis or biosensors.

Acknowledgement

Financial support from Ratchadaphisaksomphot Endowment Fund of Chulalongkorn University is gratefully acknowledged.

References

[1] R.M. Blanco, P. Terreros, M. Fernández-Pérez, C. Otero, G. Diáz-González, J. Mol. Catal. B: Enzym. 30 (2004) 83.
[2] S.S. Caramori, K.F. Fernandes, Proc. Biochem. 39 (2004) 883.
[3] K.F. Fernandes, C.S. Lima, F.M. Lopes, C.H. Collins, Proc. Biochem. 39 (2004) 957.
[4] J. Cheng, S.M. Yu, P. Zuo, Water Res. 40 (2006) 283.
[5] D. Goradia, J. Cooney, B.K. Hodnett, E. Magner, J. Mol. Catal. B: Enzym. 32 (2005) 231.
[6] Y.-C. Lai, S.-C. Lin, Proc. Biochem. 40 (2005) 1167.
[7] P.H. Panya, R.V. Jasra, B.L. Newalkar, P.N. Bhatt, Micropor. Mesopor. Mater. 77 (2005) 67.
[8] Z. Dai, H. Ju, H. Chen, Electroanalysis 17 (2005) 862.
[9] X.-L. Luo, J.-J. Xu, W. Zhao, H.-Y. Chen, Sens. Actuators B 97 (2004) 249.
[10] Q. Xu, C. Mao, N.-N. Liu, J.-J. Zhu, J. Shen, React. Funct. Polym. 66 (2006) 863.
[11] J.-Z. Xu, Y. Zhang, G.-X. Li, J.-J. Zhu, Mater. Sci. Eng. C 24 (2004) 833.
[12] Z.-X. Zhao, M.-Q. Qiao, F. Yin, B. Shao, B.-Y. Wu, Y.-Y. Wang, X-Sh. Wang, X. Qin, Sh. Li, L. Yu, Q. Chen, Biosens. Bioelectron. 22 (2007) 3021.
[13] H. Takahashi, B. Li, T. Sasaki, C. Miyazaki, T. Kajino, S. Inagaki, Micropor. Mesopor. Mater. 44/45 (2001) 755.
[14] A.S.M. Chong, X.S. Zhao, Appl. Surf. Sci. 237 (2004) 398.
[15] H. Ma, J. He, D.G. Evans, X. Duan, J. Mol. Catal. B: Enzym. 30 (2004) 209.
[16] H.H.P. Yiu, P.A. Wright, N.P. Botting, Micropor. Mesopor. Mater. 44/45 (2001) 763.
[17] J.F. Díaz, K.J. Balkus Jr., J. Mol. Catal. B: Enzym. 2 (1996) 115.
[18] Y.-J. Han, J.T. Watson, G.D. Stucky, A. Butler, J. Mol. Catal. B: Enzym. 17 (2002) 1.
[19] J. He, X. Li, D.G. Evans, X. Duan, C. Li, J. Mol. Catal. B: Enzym. 11 (2000) 45.
[20] A.S. Maria Chong, X.S. Zhao, Catal. Today 93–95 (2004) 293.
[21] A.S. Maria Chong, X.S. Zhao, Appl. Surf. Sci. 237 (2004) 398.
[22] K. Szymańska, J. Bryjak, J. Mrowiec-Białoń, A.B. Jarzębski, Micropor. Mesopor. Mater. 99 (2007) 167.
[23] S. Solis, J. Painagua, J. Martínez, M. Asomoza, J. Sol-Gel Sci. Technol. 37 (2006) 125.
[24] J.L. Gómaz, A. Bódalo, E. Gómaz, J. Bastid, A.M. Hidalgo, M. Gómaz, Enzym. Microb. Technol. 39 (2006) 1016.
[25] M.H. Entezari, C. Pétrier, Ultrason. Sonochem. 12 (2005) 283.
[26] D.P. Markris, J.T. Rossiter, Food Chem. 77 (2002) 177.
[27] S.S. Rosatto, L.T. Kubota, G.O. Neto, Anal. Chim. Acta 390 (1999) 65.
[28] L.D. Mello, M.D.P.T. Sotomayor, L.T. Kubota, Sens. Actuators B 96 (2003) 636.
[29] L.D. Mello, A.A. Alves, D.V. Macedo, L.T. Kubota, Food Chem. 92 (2005) 515.
[30] J. Deere, E. Magner, J.G. Wall, K. Hodnett, J. Phys. Chem. B 106 (2002) 7340.
[31] D.H. Cho, T.S. Change, S.K. Ryu, Y.K. Lee, Catal. Lett. 64 (2000) 227.
[32] D. Zhao, Q. Huo, J. Feng, B.F. Chmelka, G.D. Stucky, J. Am. Chem. Soc. 120 (1998) 6024.
[33] J.S. Lettow, Y.J. Han, P. Schmidt-Winkel, P. Yang, D. Zhao, G.D. Stucky, Langmuir 11 (2000) 8291.
[34] B. Halpin, R. Pressey, J. Jen, M. Mondy, J. Food Sci. 54 (1989) 644.
[35] H. Takahashi, B. Li, T. Sasaki, C. Miyazaki, T. Kajino, S. Inagaki, Chem. Meter. 12 (2000) 3301.
[36] C. Montiel, E. Terrés, J.-M. Domínguez, J. Aburto, J. Mol. Catal. B: Enzym. 48 (2007) 90.
[37] K. Rezwan, L.P. Meier, L.J. Gauckler, Biomaterials 26 (2005) 4351.
[38] T.-Y. Lin, C.-H. Wu, J.D. Brennan, Biosens. Bioelectron. 22 (2007) 1861.
[39] K.A. Carrodo, S.M. Macha, D.M. Tiede, Chem. Mater. 16 (2004) 2559.